J. Faleskog, K. Zaremba*, F. Nilsson*, and H. Öberg**

An Investigation of Two- and Three-Dimensional Elasto-Plastic Crack Growth Experiments

REFERENCE Faleskog, J., Zaremba, K., Nilsson, F., Öberg, H., **An investigation of two- and three-dimensional elasto–plastic crack growth experiments**, *Defect Assessment in Components – Fundamentals and Applications*, ESIS/EGF9 (Edited by J. G. Blauel and K.-H. Schwalbe) 1991, Mechanical Engineering Publications, London, pp. 333–343.

ABSTRACT The applicability of the J-integral for characterisation of crack growth in realistic geometries and under complex loading conditions has been investigated by experiments on different types of specimens. Both conventional type specimens (three-point bend bars and single edge notched panels) and slightly curved plates with surface cracks were tested, the latter under combined bending and tension. J was evaluated by three-dimensional non-linear FEM calculations. The J-values at initiation of crack coincided quite well for all three-dimensional tests, while the comparison with the two-dimensional tests was more uncertain.

Introduction

In most metallic materials of practical interest, initiation of crack growth and subsequent growth usually take place after considerable plastic deformation has occurred. The formulation of the conditions under which a crack will start to grow and how the ensuing growth can be predicted still remains one of the central areas in fracture research. One of the most widely used parameters for characterising the crack tip state under elasto-plastic conditions is the J-integral. Numerous experimental investigations have been carried out in order to explore its relevance to crack growth description. However, the majority of these studies have been concerned with a few geometries, suitable for laboratory work and materials testing. Much research remains in order to verify the transferability of results obtained from such specimens to geometries encountered in actual failure assessment situations.

The main object of the present investigation is to compare results obtained from several experiments on large specimens containing surface cracks with each other and also with results from typical laboratory specimens. Similar investigations have been carried out by Kordisch and Sommer **(1)**, who found that the J-integral alone is not sufficient to characterise crack growth. They found that the amount of constraint affected the critical J-values.

Another question that has not been sufficiently studied is the effect of more complicated loading situations. In most experimental investigations only one loading system is applied so that at least approximately a state of proportional loading prevails. Klasén and Kaiser **(2)** performed experiments on nominally

* Department of Solid Mechanics, Royal Institute of Technology, S-100 44 Stockholm, Sweden.

two-dimensional configurations where a deformation-controlled bending moment was applied simultaneously with a force-controlled tensile load. By varying the proportions between the tensile and the bending load they investigated if the J versus Δa curves were influenced by the different loading histories. Their main conclusion was that the J–Δa curves were, for practical reasons, the same. In the present work, load history effects of this kind are investigated for three-dimensional crack configurations.

Material and experimental arrangements

The material used in all experiments was a pressure vessel steel (2 1/4 Cr 1 Mo, yield stress 255 MPa, $R_m = 480$ MPa at the test temperature) taken from a decommissioned pressure vessel previously operated by Neste Oy in Helsinki, Finland. This material has been the base material in a large cooperative Scandinavian fracture mechanics project (Rintamaa *et al.* **(3)**) and has been extensively tested with respect to its fracture properties.

The specimens were of three basic types: a single-edged notched tensile (SEN) specimen (Fig. 1a), a three-point bend (3PB) specimen (Fig. 1(b)), and a plate specimen with a surface crack (SCT, Fig. 1(d)). The SEN and the 3PB specimens are here termed two-dimensional specimens although the tests do not necessarily comply with a truly two-dimensional state. The SCT specimens will in turn be termed three-dimensional.

In order to study the effects of side-grooves, some of the two-dimensional specimens were grooved. The thickness of the two-dimensional specimens was 25 mm which was considered sufficient to at least make the 3PB tests valid according to the requirements of ASTM E-813. In order to maximize the difference between the SEN and the 3PB specimens, the SENs were loaded by clamping the edges with jaws that prohibited rotational movements. This constraint caused a reaction in the form of a bending moment to be present besides the tensile load. Strain was measured by gauges placed along a line near the edge of the specimen. By use of the stress–strain curve the stresses acting on the edge of the specimen were calculated. Moment and membrane loads were then obtained by integration. By comparing the membrane force determined in this way, with the total force measured by a load cell in the testing machine, a check on this procedure could be made.

The loading of the specimen was done in accordance with ASTM E-813 with partial unloadings made in order to facilitate the crack growth determination by the compliance technique. The determination of J was for the bend specimens performed according to ASTM E-813. Thus J is given by

$$J = \frac{K_I^2(1-\nu^2)}{E} + \frac{2}{t(W-a_0)} \int P \, d\delta_{pl} \tag{1}$$

Here K_I is the stress-intensity factor, P the load, δ_{pl} the plastic part of the displacement of the loading point, a_0 the initial crack length, W the width, and

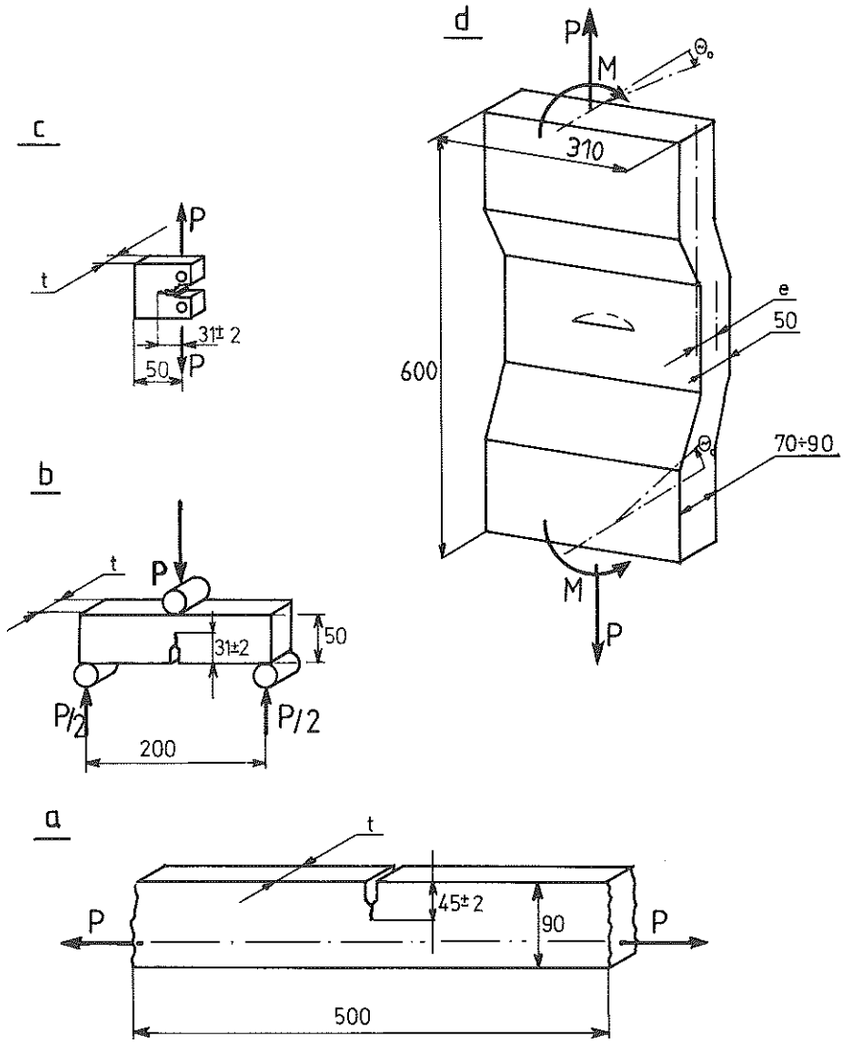

Fig 1 Different specimen types used

t the thickness of the specimen. For the SEN specimens there is no standardised procedure for experimental J evaluation. A procedure developed by Kaiser **(4)** for determination of J under combined tension and bending was used. J is then determined by

$$J = \frac{K_I^2(1-\nu^2)}{E} + \int \frac{\eta M}{W-a} \, d\theta_{pl} + \int \frac{\eta N}{W-a} \, d\delta_{pl} \tag{2}$$

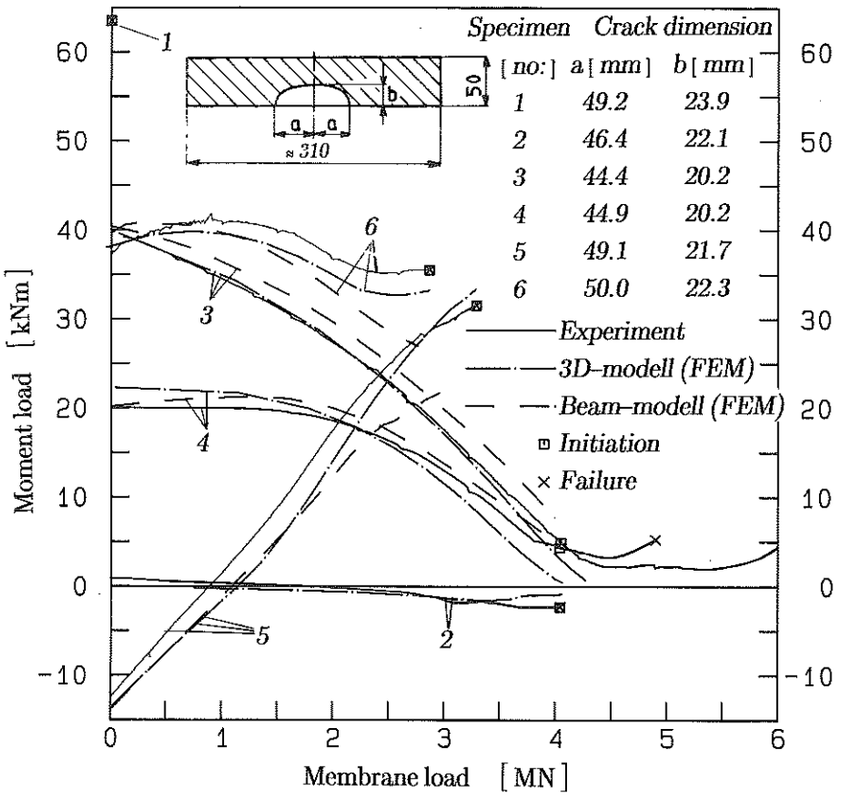

Fig 2 Moment versus normal force from testing and predictions

where η is a non-dimensional factor depending on the current excentricity of the loading and is given in **(4)**. M is the bending moment, N the tensile load, and θ_{pl} the plastic part of the rotation.

A series of experiments with the more complex crack geometry (SCT) and loading was also performed. The specimen is a slightly curved 50 mm thick plate, the midpoint of the cracked section being offset a distance e compared to the midpoints of the ends of the specimen. The object of this design was to induce a bending moment tending to open the crack. The specimen ends were welded to circular 60 mm thick plates which in turn were mounted by screws along the periphery to a servo-hydraulic testing machine. In addition to the tensile loading the specimens were mounted to the machine with an initial slant angle θ_0 thus inducing an initial bending moment. The specimens were thus subjected to two loading systems, where the applied tension could be regarded as a primary loading which induces both tensile and bending loads. The initial displacement could be considered as secondary bending load. By varying the offset e and the angle θ_0 different M–N histories could be obtained

where M and N are the moment and the membrane loads respectively as referred to the cracked section. One of the objects of this investigation was to study whether the path to a point in the M–N diagram had any influence on the crack initiation behaviour. In the course of planning, a simple beam model of the system was considered. The M–N histories for different e and θ_0 were obtained by running this model with the program system ABAQUS **(5)** taking plastic behaviour and large deformation effects into account. The results of these calculations for the four experiments are shown in Fig. 2 together with the behaviour observed during the actual experiments. As can be seen the agreement between the predicted and the observed behaviour is good, except perhaps at the highest load levels where plastic effects relax the bending moment very rapidly. In addition to these four experiments two tests were made with the offset e equal to zero. One of these was tested under pure tension, while the other was tested under three-point bending.

The crack was produced by first machining a semi-circular slit perpendicular to the surface. After fatigue loading in bending the cracks assumed approximately semi elliptical shapes. The depth and length of the cracks are given in Fig. 2.

During the testing the specimens were instrumented with strain-gauges at different locations for measurement of loads and crack length. The crack length measurements were made by partial unloadings and strain measurements in the vicinity of the crack.

All testing was performed at room temperature ($\approx 21°C$) which is approximately in the middle of the transition interval for the fracture properties of the material. The NDT temperature as measured by Charpy 'V' testing is about 10°C.

FEM-modelling

The finite element calculations were performed with the program system ABAQUS **(5)**. In all calculations the material was assumed to be elastic–plastic and to obey the von Mises flow criterion with its associated flow rule. The hardening behaviour was taken as isotropic with a piece-wise linear approximation of the uniaxial tensile test curve. The J-integral calculations were performed with the routines for this purpose built into ABAQUS. For all calculations twenty noded solid brick elements were employed. The rather accentuated grading of the mesh division was accomplished by the technique with multi-point constraints available in ABAQUS.

Since a number of rather complicated finite element models had to be developed, it was judged worthwhile to develop a special element generating program. This program was based on the idea of generating orthogonal meshes by means of conformal mapping suggested by Tsamasphyros and Giannakopulos **(6)**. An example of a generated mesh containing 745 elements and 3983 nodes is shown in Fig. 3. The generating program allowed for easy

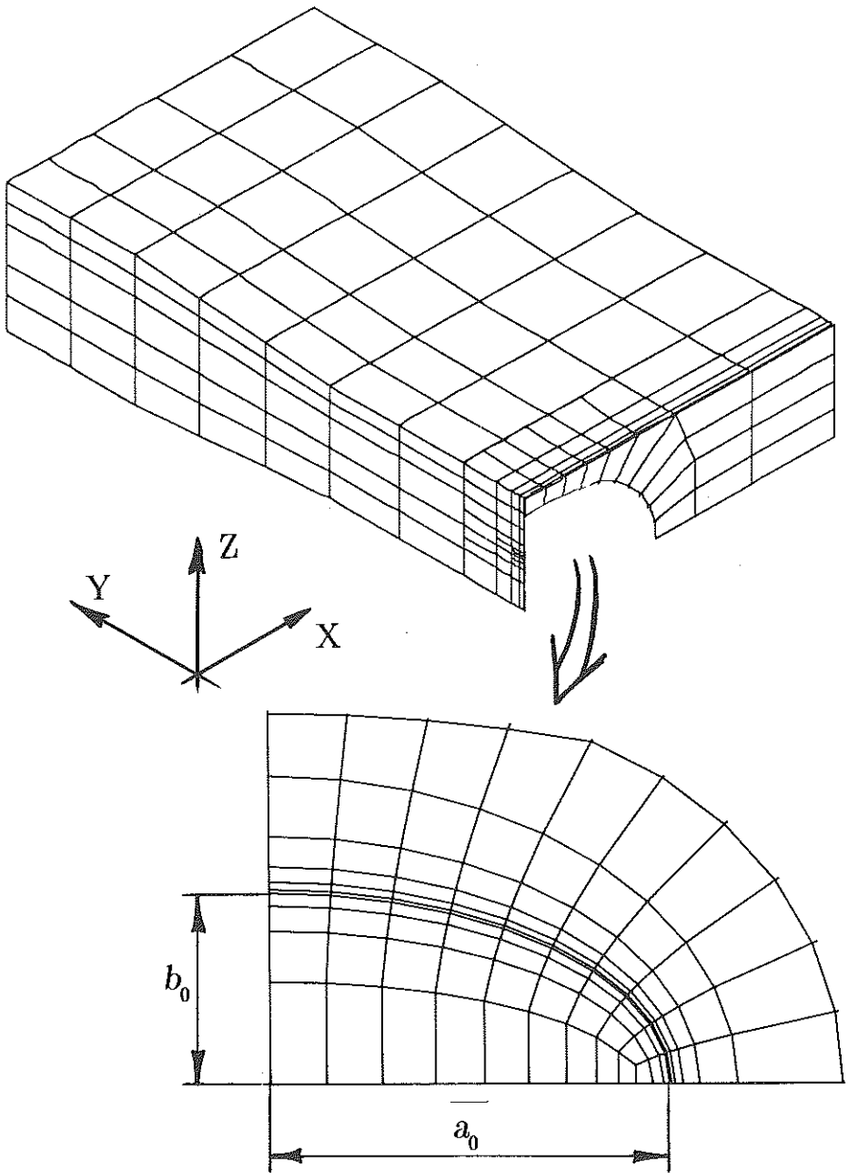

Fig 3 Finite element mesh for three-dimensional calculations

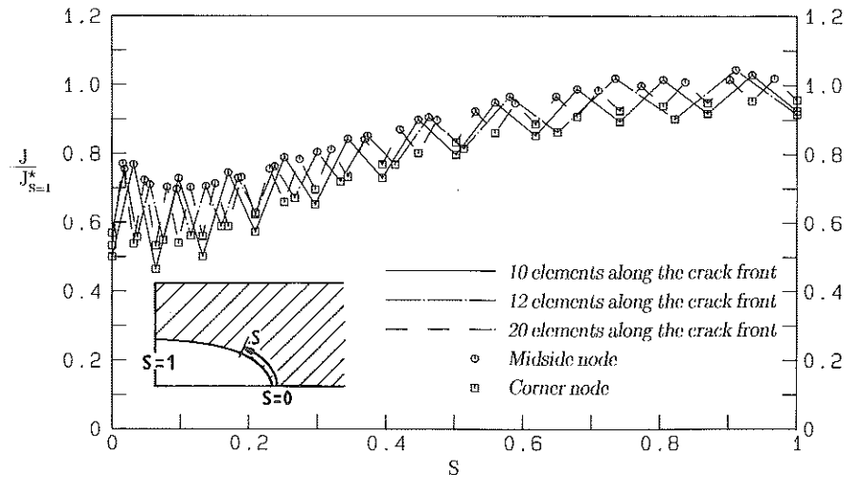

Fig 4 Non-weighted *J* values along the crack front for different meshes and elastic conditions

generation of models with successive refinements of the mesh division in the vicinity of the crack border.

Because of symmetry only a quarter of the specimen needed to be modelled. On the symmetry planes the appropriate conditions were assumed. At the loaded boundary the displacements were assumed to be prescribed as $u_x = u_z = 0$ and $u_y = f(t)$, thus simulating a clamped and rigidly moving boundary plane. Some sensitivity studies were undertaken in order to assess the effects of the finite stiffness of the mounting plates. These calculations revealed that the flexibility of the mounting device could safely be disregarded.

All calculations were performed taking non-linear geometry effects into account. This proved necessary because of the special type of experimental arrangements where the bending moment is significantly affected by the finite deformation.

For one of the tests (No. 5, Fig. 2) crack closure occurred during the initial tilting of the boundaries. For this case gap elements were used in order to simulate closure. Gap elements were also used to simulate the loading conditions in the pure bending test (No. 1) where the specimen was loaded in three-point bending. Friction effects were neglected.

The path-independence of the *J*-values was reasonable for all specimens except for the one tested under three-point-bending (experiment No. 1). The path-independence for this specimen proved to be poor when the failure load was reached and high plastic deformation was present. The results for the bend specimen were considered not to be reliable and will not be presented here.

It turned out that the *J*-values oscillated along the crack front (see Fig. 4). The values differed depending on whether they were evaluated at the corner

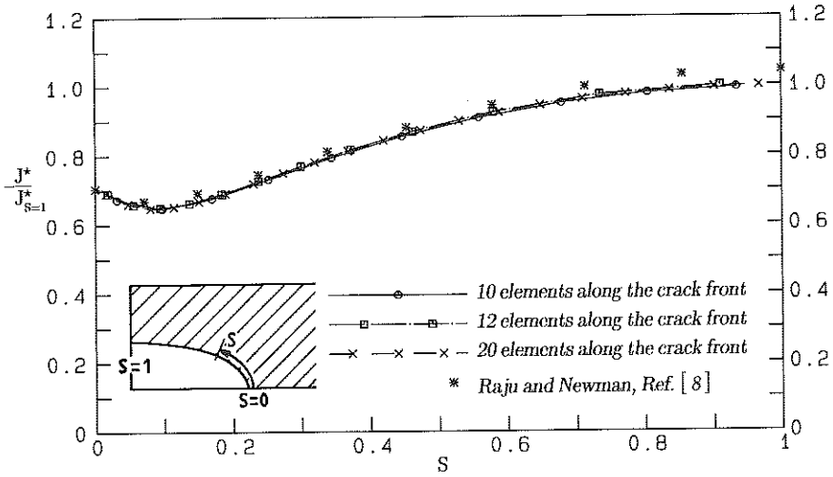

Fig 5 Weighted *J*-values compared with the results of (8)

nodes or at the midside nodes. This behaviour has been noted by other authors. Therefore, Kozluk *et al.* **(7)** have suggested a method of constructing a weighted average for the J value according to a scheme analogous to the determination of consistent nodal forces, i.e.

$$J^* = 1/6(J_{\text{corner1}} + 4J_{\text{midside}} + J_{\text{corner2}}) \tag{3}$$

This weighting scheme was used also in the present investigation. As a test, linearly elastic calculations for the purely tensile geometry were performed with increasingly fine subdivisions of elements in the vicinity of the crack front. The resulting non-weighted J values are shown in Fig. 4. The J-integral, evaluated in planes perpendicular to the crack-front in each node is normalised against the weighted value J^* in the deepest point of the crack, where $s = 1$ (see Fig. 5). As can be seen the oscillations decrease with increasing number of elements. The weighted averages, shown in Fig. 5, coincide rather well with each other and also with the results of Raju and Newman **(8)**. Based on these results it was judged that a division corresponding to the coarsest one in Fig. 4 should give sufficiently accurate J-values in the elasto-plastic evaluations of the experiments. This was important since a full calculation of a test requires about 50 CPU-hours on one processor of an Alliant FX computer.

Discussion of experimental and numerical results

In all of the two-dimensional tests considerable amounts of stable crack growth occurred. In Fig. 6 the J–Δa curves from representatative tests of each of the two-dimensional types are plotted. Here, open circles signify crack lengths observed by direct measurement on the fractured surface, while the other points represent evaluations by the compliance method. Some uncer-

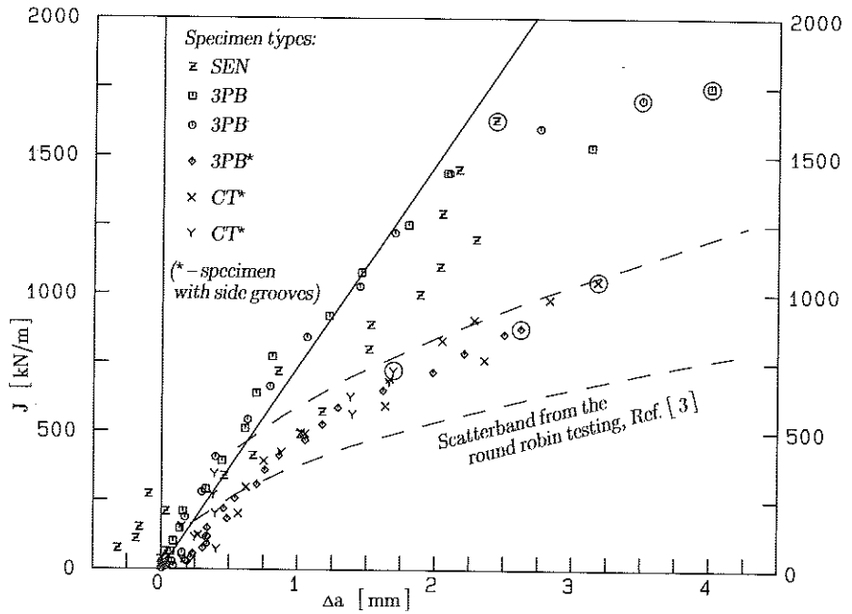

Fig 6 J_R-values for two-dimensional tests

tainty regarding the crack length measurement was evident especially for the SEN specimen where the experience with the compliance method was limited. In view of this, the agreement between the results from tests on non-grooved specimens is acceptable. In Fig. 6 the results from one side-grooved 3PB specimen are shown and it is noted that the J–Δa values are considerably lower than for the non-grooved tests. Figure 6 also contains the mean curve from the round robin testing of the same material at 50°C reported in **(3)**. These results were also obtained by using sidegrooved CT specimens and agree fairly well with the sidegrooved 3PB experiment. It may be noted that all observed points fall to the right of the blunting line. This type of behaviour as well as the lowering of the J_R–Δa curve caused by grooving the specimens were also observed in **(1)**. Judging from the appearance of the J–Δa curves at small growth increments, it is difficult to unambiguously determine a J_{Ic} value for the present material. An evaluation according to the ASTM E-813 proved to be impossible to perform.

The three-dimensional experiments were characterised by the fact that after a rather extensive plastic deformation, unstable growth occurred immediately after initiation for the majority of the tests. It was only in two of the six experiments (Nos 3 and 4 in Fig. 2) that any appreciable stable crack growth occurred. For these, the point of crack growth initiation was estimated by considering the unloading compliance measured by the strain gauges in the vicinity of the surface crack. All the experiments were evaluated by FEM in

the manner described above. In Fig. 7 the J-distribution along the crack front at the estimated initiation load is shown for all six three-dimensional tests. As can be seen the maximal J-value for each test falls within a reasonably narrow scatterband marked in the figure. This also indicates that the loading history is of minor significance for the crack growth initiation event if J is evaluated properly taking the entire process into account. In fact, for the present set of

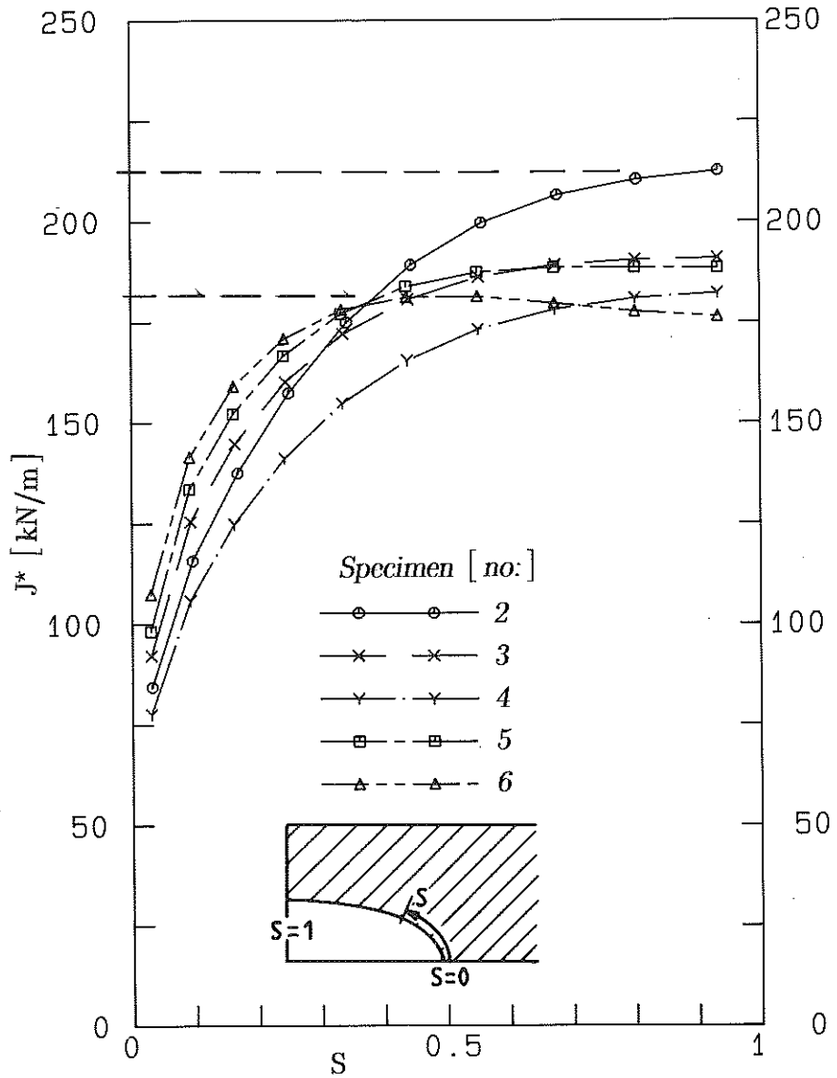

Fig 7 *J*-values at critical loads for three-dimensional tests

experiments it can be judged directly from Fig. 2 that the secondary loading is of minor importance. Comparing, e.g., tests Nos 5 and 6 which were of identical geometry, it is noted that the large difference in initial secondary moment does not affect the point of failure very much.

Concluding remarks

Crack growth initiation occurred at approximately the same maximal J-value (180–214 kN/m) for the three-dimensional experiments. Thus it appears that J can serve as crack tip characterising parameter in three-dimensional situations. However, it was difficult to unambiguously find a corresponding value from the two-dimensional testing, thus casting some doubts on the transferability of J_c-results from testing of laboratory type specimens. Although the results from nongrooved bend and tension testing, respectively, agreed, the insertion of sidegrooves lowered the critical J-values to levels closer to the ones where initiation occurred in the three-dimensional tests.

Acknowledgements

This work was funded by a grant jointly from the Swedish Nuclear Power Inspectorate (SKI) and the Nordic Liaison Committee for Atomic Energy (NKA). We are grateful for this support and also wish to thank Professor B. Andersson and Dr A. E. Giannakopoulos for helpful advice during the course of this project.

References

(1) KORDISCH, H. and SOMMER, E. (1988) Three-dimensional effects affecting the precision of life-time predictions, *ASTM STP 969*, (Edited by T. A. Cruse), pp. 73–87, ASTM, Philadelphia.

(2) KLASEN, B. and KAISER, S. (1988) Studies of stable crack growth under two independent loads, *Int. J. of Fracture*, **36**, 259–273.

(3) RINTAMAA, R., WALLIN, K., IKONEN, K., TÖRRÖNEN, K., TALJA, H., KEINÄNEN, H., SAARENHEIMO, A., NILSSON, F., SARKIMO, M., WÄSTBERG, S., and DEBEL, C. (1989) Prevention of catastrophic failures in pressure vessels and piping, Nordic Liaison Committee for Atomic Energy, *Final report MAT* **570**.

(4) KAISER, S. (1985) The J-integral and tearing modulus for a SEN specimen under bending and tension, *Engng Fracture Mech.*, **22**, 737–749.

(5) ABAQUS (1988) *User's Manual* **4.7**, Hibbit, Karlsson, and Sorensen Inc., Providence Rhode Island.

(6) TSAMASPHYROS, G. and GIANNAKOPOULOS, A. E. (1986) Automatic optimum mesh around singularities using conformal mapping, *Engng Fracture Mech.*, **23**, 507–520.

(7) KOZLUK, M., MANNING, B. M., MISRA, A. S., LIN, T. C., and VIJAY, D. K. (1988) Linear elastic solutions for long radius piping elbows with curvilinear throughwall cracks, ABAQUS, *User's Conference Proceedings*, Newport, Rhode Island, 197–210.

(8) RAJU, I. S. and NEWMAN Jr, J. C. (1979) Stress intensity factors for a wide range of semi-elliptical surface cracks in finite-thickness plates, *Engng Fracture Mech.*, **11**, 817–829.